Journal of Alloys and Compounds 764 (2018) 136–141

Contents lists available at ScienceDirect

Journal of Alloys and Compounds

journal homepage: http://www.elsevier.com/locate/jalcom

EPR response of yttria micro rods activated by europium

S.C. Santos*, O. Rodrigues Jr., L.L. Campos

Instituto de Pesquisas Energeticas e Nucleares – IPEN, Av. Prof. Lineu Prestes 2242, Cidade Universitaria, Sao Paulo, Brazil

ARTICLE INFO

Article history:
Received 5 April 2018
Received in revised form
5 June 2018
Accepted 6 June 2018
Available online 15 June 2018

Keywords:
Yttria
Europium oxide
Rare earths
Lanthanides
EPR
Radiation dosimetry
Rods
Ceramic processing

ABSTRACT

Rare earth (RE) materials present excellent properties, which importance is recognized worldwide. Innovation approaches in energy, medicine, communication, transportation, militarism, and radiation dosimetry consist in RE based materials. As yttrium oxide (Y_2O_3) exhibits intrinsic lattice characteristics that enable doping with others RE elements (Y_2O_3:RE), new materials with promising characteristics can be developed. This work aims to evaluate EPR response of europium-yttria (Y_2O_3:Eu) rods obtained by bio-prototyping. Ceramic rods containing up to 10 at.%Eu were irradiated with gamma doses from 0.001 to 150 kGy and evaluated by Electron Paramagnetic Resonance (EPR) at room temperature with X-band EPR. Based on results, Y_2O_3:Eu rods with 2 at.%Eu exhibited the most significant response, in which linear behavior arose from 0.001 up to 50 kGy. Fading and thermal annealing evaluations revealed that 2 at%.Eu improved dosimetric characteristics of yttria remarkably. These innovative findings afford that Y_2O_3:Eu is a promising material for radiation dosimetry.

1. Introduction

The Fourth Industrial Revolution characterized as global transformation in which digital, physical, chemical, and biological sciences converge, is in progress due to materials development [1–3]. Development of new dosimetric materials is inserted into mission-oriented innovation policy agenda, which means identifying and articulating new approaches to galvanize research-development, production, distribution, and consumption patterns trough sectors [4].

As rare earths (REs) exhibit expressive properties their use even if in low concentration (atomic percentage) lead to improvement of materials proprieties. These new materials become suitable for application in highly advanced technologies as dosimetry materials. Dysprosium doped calcium sulphate ($CaSO_4$:Dy) used as thermoluminescent dosimeter is applied for beta [5], gamma [6], X [7], electrons [8], photons [9], UV [10] and laser dosimetry [11]. The $CaSO_4$:Dy dosimeter exhibits excellent reproducibility, high sensitivity [12], AO [13] and EPR [14] response. Therefore, the use of rare earths as materials for dosimetry applications is on frontier knowledge.

Yttria (Y_2O_3) is a promising material for radiation dosimetry due to its unique proprieties as, density of 5.02 g cm^{-3}, refractive index over 1.9, melting point of 2400 °C, band gap of 1.6eV, Young's modulus of 160 GPa, and cubic C-type lattice composed by Ia_3 space group, sixteen formula units per unit cell, coordination number (N) of 6, and two points symmetry (S_6, C_{3i}) and C_2 [15,16]. Nian Xu et al. [17] reported that cubic structure of Y_2O_3 is less closely packed, exhibiting large vacancies of Y and O planes. These vacancies enable incorporation of RE ions into yttria host and formation of highly luminescent materials (Y_2O_3:RE) can be achieved.

Spectroscopic characteristics of yttria are improved according to processing parameters such as, RE dopant concentration [18], synthesis method [18], microstructure [19], crystallite-particle size [20], and shaping [21]. Upon applications yttria is used as, thermal coatings [22], catalysts [23], special alloys, biomaterials [24], scintillators [25], luminescent devices [26], membranes [27], gas burners [28], sintering aid [29], capacitors [30], nanocomposites [31], and reinforcement [32]. In addition, yttria is a promising material for dosimetry [33]. Even though yttria presents reliable proprieties, being used in many applications, few studies on massive processing of this promising rare earth have been carried out.

Recently, our group reported approaches on bio-prototyping of rare earth based ceramics [19,28,34–37], including yttria based rods with potential application in radiation dosimetry. Ceramic

* Corresponding author.
E-mail address: silas.cardoso@alumni.usp.br (S.C. Santos).

https://doi.org/10.1016/j.jallcom.2018.06.063
0925-8388/

rods of yttria and europium-yttria with dense microstructure and homogeneous shape-size were obtained by sintering at 1600 °C for 4 h in air atmosphere [38,39]. As a step forward to obtain a new dosimeter material, the present study purposes to evaluate EPR response of europium-yttria rods as a function of ionizing irradiation dose, in which dosimetry parameters as EPR spectra, dose-response, fading, and thermal annealing are analyzed and discussed.

2. Experimental

Europium-yttria rods (Y_2O_3:Eu) were produced by bio-prototyping according our recent study [38], which process is illustrated in Fig. 1. Europium content was from 0.5 up to 10 at.%. The morphology and size evaluation of ceramic rods were performed by optical microscopy (OM, Nikon SMZ1270). Besides, microstructure formation was observed by scanning electron microscopy (SEM, Oxford Instruments).

Batches of four ceramic rods were irradiated with gamma source with dose range from 0.001 to 150 kGy in electronic equilibrium conditions and room temperature. Crystal defects and radicals induced by ionizing radiation were characterized by electron paramagnetic resonance at room temperature and atmosphere using X-band EPR spectrometer (Bruker EMX PLUS).

EPR spectra of samples were recorded using the following parameters: field frequency modulation of 100 kHz, microwave power of 2.5 mW, centre field at 320 mT, sweep width of 600 mT, modulation amplitude of 4G, time constant of 0.01 ms and, 10 scans. The EPR response of irradiated samples was determinated as a mean of each batch normalized by mean mass of containing samples. EPR dose response and time decay curves were plotted considering the mean of peak-to-peak amplitudes of irradiated samples.

3. Results and discussion

Formation of crystalline europium-yttria micro rods for radiation dosimetry depends on processing parameters as, synthesis route, dispersion of powders, viscosity of suspension, shaping, as well as sintering of green compacts. Bio-prototyping is an environmental friendly shaping method, in which renewable materials are used as preform to shape suspension of nano particles [38]. Stable suspensions provide green compacts constituted by high packing of particles, which avoids formation of voids during drying stage. These green compacts as sintered on suitable sintering conditions exhibit dense microstructure and substantial mechanical strength [40].

An optical image of europium-yttria micro rod (2 at.%Eu) with size of 3.335 × 2.271 mm (diameter x height) sintered at 1600 °C for 4 h is shown in Fig. 2a. The ceramic rod exhibits rough surface, and surface microstructure with grains like shape-rounded, which size is higher than 2 μm (Fig. 2b). As fractured europium-yttria micro rod presented transgranular fracture (Fig. 2c), dense-homogeneous microstructure, and containing grains with size higher than 2 μm. In our recent paper [39], in which yttria based micro rods were also produced by bio-prototyping, similar microstructural characteristics were observed. Moreover, the addition of 2 at.% europium into yttria host did not provide any substantial effect on sintering of samples.

The incorporation of europium ions into yttria gives rise to soft rearrangement of yttria crystal lattice. Since the size of ionic radius of Eu and Y is quite similar 0.098 nm and 0.092 nm, respectively, the character of incorporation is substitutive. Eu ion replaces Y ion in C_2 and S_6 sites with no significant distortion of crystal lattice, bonds to oxygen ion and, provides an oxygen vacancy, as shown in Eq. (1). However, europium excess can lead to formation of second phases, change of crystal structure and, decrease of spectroscopic characteristics as luminescence. Ranson et al. [41] reported that excess of europium into yttria provided low luminescence emission due to europium ions are located at S_6 symmetry axis of yttria host. On the other hand, using suitable concentration of doping, europium ions tend to be located at C_{3i} axis and, as a consequence provide highly luminescence emission of samples.

$$Eu_2O_3 \xrightarrow{Y_2O_3} Eu_Y + O_O^x + V_O^{\cdot\cdot} \quad (1)$$

Cubic C-type yttria is composed by YO_6 unit cells, which exhibit two oxygen vacancies located at the corners. The cell arrangement forms the structure of the YO radical situated in the outer surface of cell and bounded to crystal lattice by yttrium ion as illustrated in Fig. 3a. The interaction of YO radical with its environment is determinant on luminescence of the material. Moreover, particle size and shape is effective on YO radical behavior. As the size of particle increases, its flat surface also increases and leads to weak the interaction of YO radical with environment. Osipov et al. [42] reported that yttria powders with particle size smaller than 3 μm exhibited a broad cathode luminescence band at λ around of 437 nm. On the other hand, particles with size higher than 5 μm exhibited emission bands in blue, orange, red and infrared series.

Yttria exhibits intrinsically considerable number of vacancies,

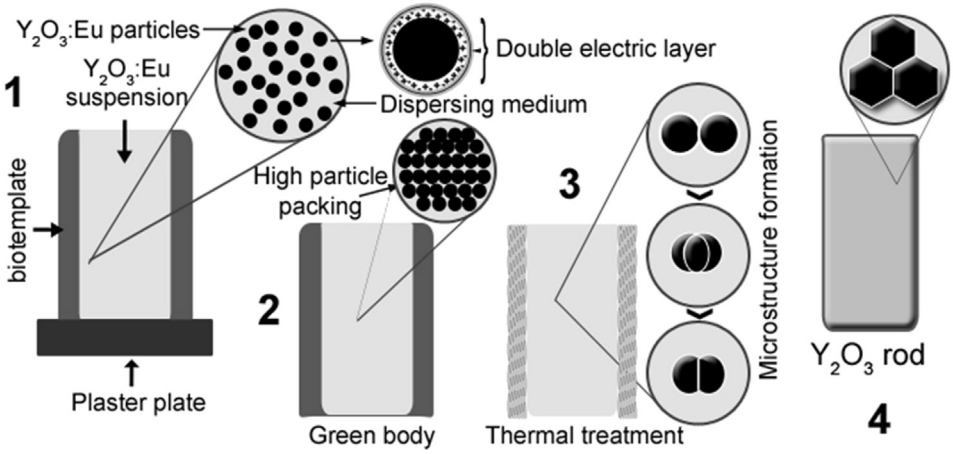

Fig. 1. Bio-prototyping of europium-yttria rods performed in this work.

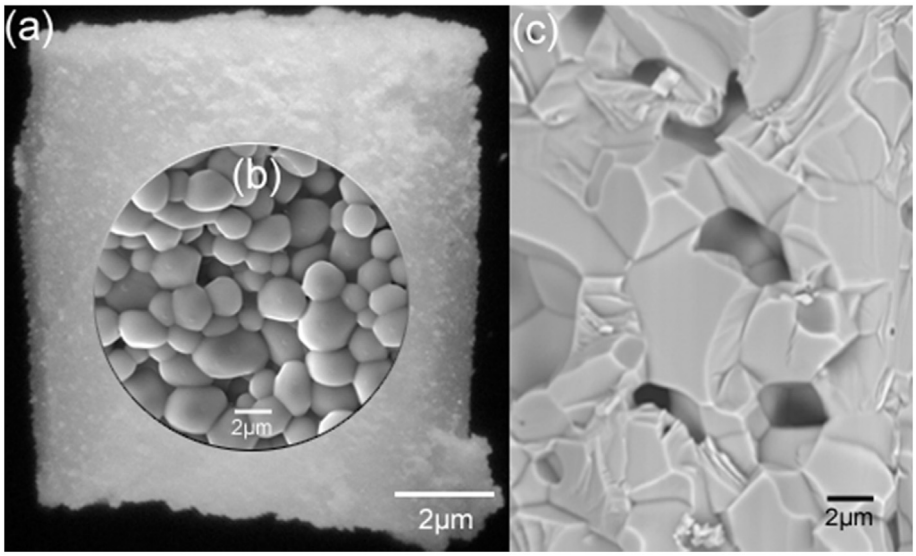

Fig. 2. Europium-yttria rod formed by bio-prototyping: (a) optical image of ceramic rod; (b) surface microstructure; (c) inner surface showing cleavage planes characteristic of fragile fracture.

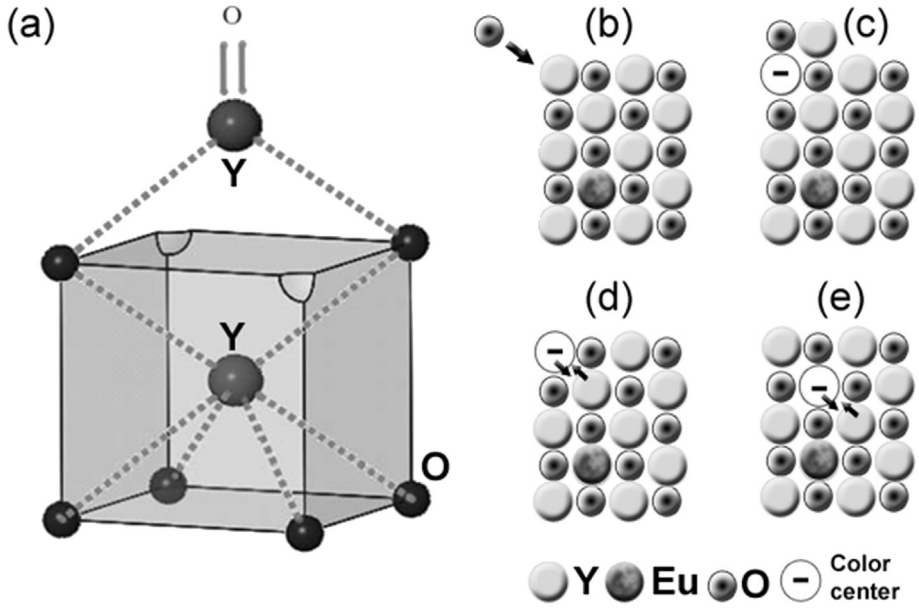

Fig. 3. Formation of color centre in yttria: (a) YO radical bonded to crystal lattice (b–d) diffusion of electron into crystal lattice.

which make favourable insertion of rare earth ions to improve host material characteristics. The incorporation of Eu ions into Y_2O_3 lattice gives rise to rearrangement of its crystal lattice i.e. formation of color centres, new induced crystal defects (point, linear, and volume). In addition, this crystal rearrangement can provide new energy levels and pairs of electrons-holes, as shown in Fig. 3b. The interaction of ionizing radiation with matter leads to development of radicals by means of unpaired electrons, which are detectable by Electron Paramagnetic Resonance (EPR). Thus, EPR is useful technique to evaluate ionizing induced defects, providing substantial information to develop new dosimetry materials.

The incorporation of europium intro yttria lattice is performed by replacing Y^{3+} ions for Eu^{3+} ions on yttria sites C_2 and C_{3i}. The effect of Eu content in promoting EPR response of Y_2O_3:Eu rods is illustrated in Fig. 4. As discussed previously [39] "pure" yttria (0% at.Eu) exhibits two distinct peaks c_1 and c_2 between 345 and 360 mT. The main peak (c_1) with g value of 2.00 and linewidth around 2.3 mT is ascribed to interstitial oxygen ion from environmental atmosphere. The c_1 peak was also observed for Y_2O_3-CaO [43] samples with g value around 2.040, and for Y_2O_3:Er [44] samples with g of 2.0415. On the other hand, c_2 peak recorded with linewidth around of 1.3 mT and g tensor of 1.969 is assigned to F^+ centre charged vacancy oxygen, which exhibits one remaining electron. In addition, C-type crystal lattice of Y_2O_3 presents intrinsic oxygen vacancies that can produce F centres close to c_2.

The incorporation of europium into yttria lattice using at least 2 at.% provided formation of two new peaks of resonance (a) and (b) as shown in Fig. 4a and b, respectively. The high intense peak c_1 (Fig. 4c) was recorded around 360 mT, with linewidth of 6 mT and g_{c1} of 2.0040. Moreover, EPR peaks addressed as (a, b, and c_2)

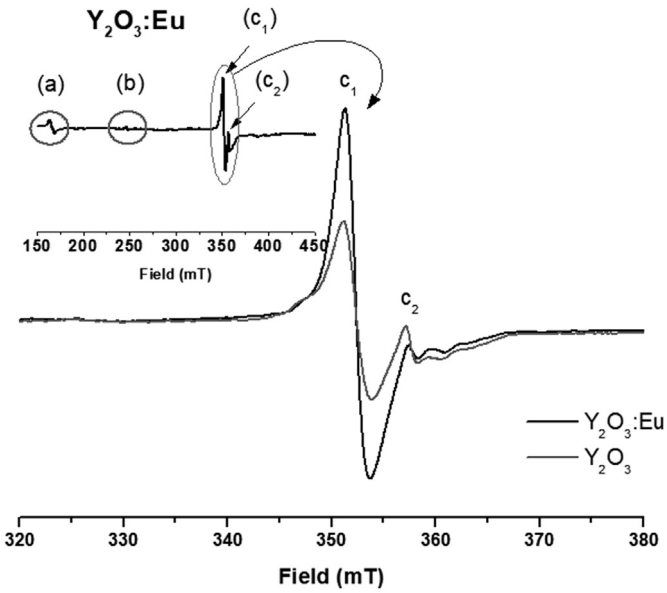

Fig. 4. EPR spectra of as sintered yttria and europium-yttria rods.

exhibited the following g values, g_a 4.2159, g_b 2.8507, and g_{c2} 1.9690. Based on results, europium incorporation into yttria host provides news resonance peaks (a, b), intensifies charge carriers and, enhances EPR response.

The aim of doping a material consists in improving its characteristics, by means of insertion of a different substance, so that the doped material exhibits a better response than its undoped state, e.g. mechanical strength, corrosion resistance, and luminescence. As yttria exhibits substantial number of vacancies, as well as a similar ionic radius like other REs, it is one of the most promising materials to form new dosimetric materials.

Doping yttria with europium (Y_2O_3:Eu) is performed by replacing Y^{3+} ions for Eu^{3+} ions on yttria lattice. The effectiveness of europium content in enhancing EPR response of yttria rods as a function of absorbed dose is illustrated in Fig. 5. As reported previously [45], yttria exhibits two distinct dose response slopes. The first range is from 1 to 100Gy, and the second is from 0.1 to 70 kGy, in which a small increase of EPR peak-to-peak was observed. Besides, a new range which might corresponds to formation of new defects is likely to begin from 70 kGy. Considering that doses from 100 kGy are extremely high for dosimetry application, this range was not evaluated in this work.

Upon on Fig. 5, it is seen that doping with 2 at.% Eu promoted a remarkable change in dose response behavior of yttria rods, in which ceramic rods exhibited a great increase of sensitiveness from 1 up to 10 kGy. The enhancement of EPR response can ascribed to suitable europium content 2 at.%Eu, phase stability, increase of luminescence centres, and higher probability of radiative recombination [46,47]. These innovative findings suggest that europium-yttria rods may be promising material for clinical dosimetry (1Gy < dose < 1 kGy), as well as industrial application (1 kGy < dose < 50 kGy). Controversially, doping with 5 and 10 at% Eu were not effective in promoting higher EPR response of micro rods.

Unsatisfactory results for micro rods samples based on 5 and 10 at%Eu can be interpreted by means of luminescence theory. Luminescent intensity/response is based on average distance between color centres. As activators concentration increases, the distance between activators decreases. As a consequence, activators will interact with each other, providing concentration quenching. On the other hand, using lower concentration as 2 at.%Eu reduces the non-radiative relaxion, increases quenching concentration and EPR response [48]. Govimdasamy et al. [16] reported that RE-doped yttria exhibits higher luminescence response as RE ions (dopant) are located at C_2 sites of host.

Based on exposed previously, doping yttria host with 2 at.% europium led to formation of a material, which dose-response behavior is quite sensitive and linearity of EPR response is from 0.001 to 10 kGy. A second formation process of new defects takes place from 10 up to 50 kGy and a third one occurs from 50 until 150 kGy. Therefore, apart from here all dosimetry discussion is on Y_2O_3:Eu samples, in which Eu content is 2 at.%.

Fading of Y_2O_3:Eu rods irradiated with doses up to 150 kGy at room temperature was evaluated considering EPR relative signal of the centre P_1 during seven days (Fig. 6). Based on results, a moderated decay behavior is observed for all irradiated samples, wherein samples irradiated with 10Gy exhibited fading of 10%, whereas those irradiated with 100 kGy presented fading around of 16%. In addition, from 96 h (four days) P_1 signal maintained at least 86% of its original signal for samples irradiated with doses around 100 kGy. Even though oxygen from atmosphere can form weak bond into Y_2O_3:Eu lattice, the new electronic defects are quite

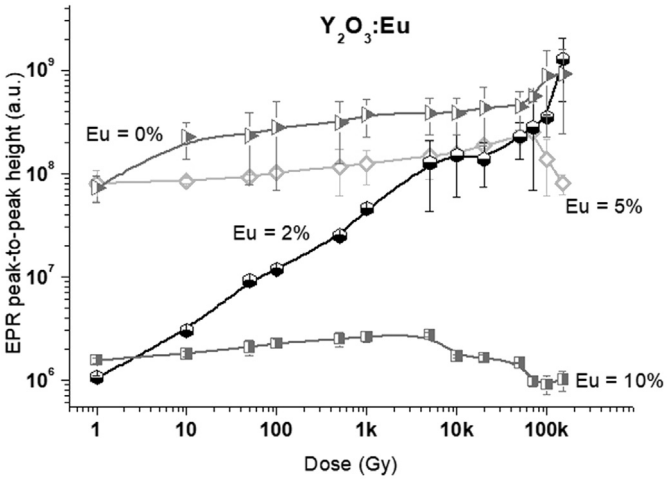

Fig. 5. Dose response behavior of Y_2O_3:Eu rods as a function of europium content.

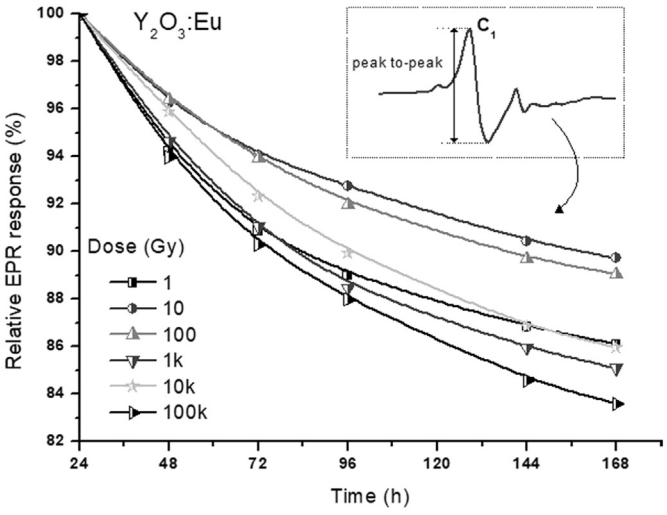

Fig. 6. Fading of EPR response of Y_2O_3:Eu rods (Eu = 2 at.%).

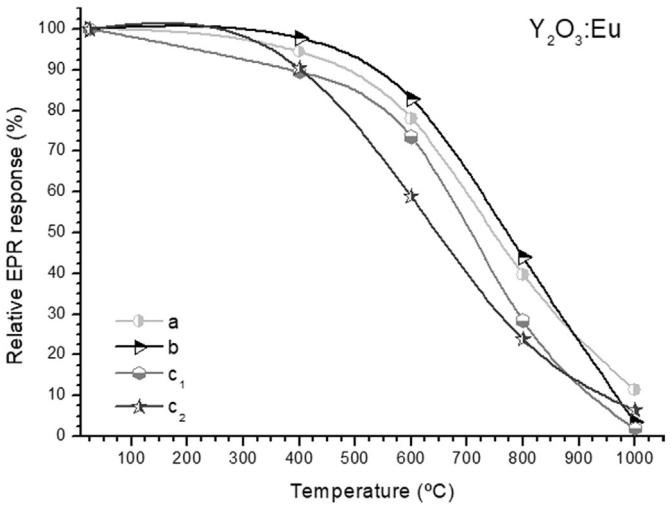

Fig. 7. Relative EPR response of paramagnetic peaks a, b, c_1, and c_2 as a function of thermal annealing of Y_2O_3:Eu rods.

stable over 168 h with maximum fading around of 16%

Fig. 7 illustrates the effect of thermal treatment on decreasing EPR response of europium-yttria rods irradiated with 150 kGy. It is observed that EPR response of peaks a, b, c_1, and c_2 is still high for thermal treatment up to 500 °C (around 75%). Controversially, Singh et al. [44] reported that Y_2O_3:Er samples irradiated with 5ky exhibited low temperature decay around 160 °C. The following EPR peaks a and b, which correspond to europium doping, presented the most stable EPR relative signal, including thermal annealing curves with similar decay. Besides, even though annealing temperature of 800 °C samples exhibited relative EPR response at least 45%. As yttria lattice exhibits great number of vacancies, F^+ centre is one of the most probable defects, i.e an electron trapped at an anion vacancy as observed by Singh [44] and Hutchison [49].

Peak c_2 showed the fastest decrease of EPR signal in the temperature range between 400 and 650 °C around 40%. Full signal cleaning was achieved at 1000 °C for c_1 peak, whereas for a, b, and c_2 peaks EPR signal of around 10% still remain. It is believed that irradiation with 150 kGy promoted deep traps that are complex to clean by thermal annealing, even though in high temperature. Using thermal annealing treatment at 1000 °C, but with longer step may be useful to achieve this goal.

4. Conclusion

Europium-yttria rods with controlled shape, size and, dense microstructure were successfully produced by bio-prototyping. Doping yttria host with 2 at.% europium led to significant improvement of EPR response of ceramic rods as a function of radiation energy. Dose response behavior of rods exhibited two distinct dose ranges, one was from 0.001 to 10 kGy, and the second was from 10 to 70 kGy. Fading stability was achieved from 144 h. Thermal annealing approaches show that defect centres of europium-yttria decay significantly by thermal treatment over 900 °C in room atmosphere. The present results reveal that europium-yttria rods exhibit innovative characteristics with potential use for radiation dosimetry.

Acknowledgements

We authors are deeply grateful to MSc. Douglas Will Leite and MSc. William Naville from The University Center of FEI; grant #2014/23621-3 from São Paulo Research Foundation (FAPESP); National Council for Scientific and Technological Development (CNPq); and Coordination for Improvement of High Degree People (CAPES).

References

[1] B. Mrugalska, M.K. Wyrwicka, Towards lean production in industry 4.0, Procedia Eng. 182 (2017) 466–473.
[2] Y. Lu, Industry 4.0: a survey on technologies, applications and open research issues, J. Ind. Inf. Integrat. 6 (2017) 1–10.
[3] F. Zezulka, P. Marcon, I. Vesely, O. Sajdl, Industry 4.0 – an introduction in the phenomenon, IFAC-PapersOnLine 49 (2016) 8–12.
[4] M. Mazzucato, C. Penna, in: The Brazilian Innovation System: a Mission-Oriented Policy Proposal, Centro de Gestão e Estudos Estratégicos, CGEE, Brasília, 2016, p. 119.
[5] T.N.O. Pinto, P.L. Antonio, L.V.E. Caldas, Measuring TL and OSL of beta radioisotopes inside a glove box at a radiopharmacy laboratory, Radiat. Meas. 46 (2011) 1847–1850.
[6] N. Shinde, N.S. Dhoble, S.C. Gedam, S.J. Dhoble, Thermoluminescence characteristics of Na-3 SO4 Cl:X (X=Ce, Dy, Mn) phosphor, Radiat. Eff. Defect Solids 169 (2014) 361–367.
[7] E.L. Correa, J.O. Silva, V. Vivolo, M.P.A. Potiens, K.A.C. Daros, R.B. Medeiros, Intensity variation study of the radiation field in a mammographic system using thermoluminescent dosimeters TLD-900 (CaSO4:DY), Radiat. Phys. Chem. 95 (2014) 116–118.
[8] J.R. Cortes, R.A. Romero, J.A. Nieto, T.R. Montalvo, Electron absorbed dose measurements in LINACs by thermoluminescent dosimeters, Appl. Radiat. Isot. 83 (2014) 210–213.
[9] S. Chatterjee, A.K. Bakshi, R.A. Kinhikar, G. Chourasiya, R.K. Kher, Response of CaSO4:Dy phosphor based TLD badge system to high energy electron beams from medical linear accelerator and estimation of whole body dose and skin dose, Radiat. Meas. 44 (2009) 257–262.
[10] J. Roman, T. Rivera, I.B. Lozano, R. Sosa, G. Alarcon, Luminescent characteristics of CaSO4:Dy films obtained by spray pyrolysis method, Appl. Radiat. Isot. 70 (2012) 1403–1406.
[11] S. Chaurasia, M. Kumar, A.K. Poswal, D.S. Munda, L.J. Dhareshwar, R.K. Kher, G. Chourasiya, Comparison of thermo-luminescent detectors and X-ray vacuum detectors for measurement of X-ray yield from gold plasma produced by a sub-nanosecond Nd:glass laser, Nucl. Instrum. Meth. A 595 (2008) 395–400.
[12] A. Piaskowska, B. Marczewska, P. Bilski, A. Mandowski, E. Mandowska, Photoluminescence measurements of LiF TL detectors, Radiat. Meas. 56 (2013) 209–212.
[13] A.K. Bakshi, S.N. Jha, L. Olivi, D.M. Phase, R.K. Kher, D. Bhattacharyya, X-ray absorption spectroscopy and X-ray photoelectron spectroscopy studies of CaSO4 : Dy thermoluminescent phosphors, Nucl. Instrum. Meth. B 264 (2007) 109–116.
[14] B. Sanyal, V. Natarajan, S.P. Chawla, A. Sharma, TL and EPR studies of CaSO4: Dy phosphor to investigate its efficacy in measurement of food irradiation dose at sub-ambient temperatures, Radiat. Meas. 45 (2010) 899–905.
[15] S.C. Santos, O.J. Rodrigues, L.L. Campos, Advances in Colloidal Processing of Rare Earth Particles, Current Smart Materials, 2017.
[16] A. Govindasamy, C. Lv, H. Tsuboi, M. Koyama, A. Endou, M. Kubo, E. Broclawik, A. Miyamoto, A theoretical study of the effect of Eu ion dopant on the electronic excitations of yttrium oxide and yttrium oxy-sulphide, Jpn. J. Appl. Phys. 1 (45) (2006) 5782–5785.
[17] Y.N. Xu, Z.Q. Gu, W.Y. Ching, Electronic, structural, and optical properties of crystalline yttria, Phys. Rev. B 56 (1997) 14993–15000.
[18] D.V. Tolstikova, M.D. Mikhailov, V.M. Smirnov, Features of the synthesis of nanoparticles of yttrium oxide Y2O3:Nd, Russ. J. Gen. Chem. 84 (2014) 2043–2044.
[19] S.C. Santos, C. Yamagata, A.C. Silva, L.F.G. Setz, S.R.H. Mello-Castanho, Yttrium disilicate micro-cellular architecture from biotemplating of Luffa cylindrica, J. Ceram. Sci. Technol. 5 (2014) 203–208.
[20] W.N. Wang, W. Widiyastuti, T. Ogi, I.W. Lenggoro, K. Okuyama, Correlations between crystallite/particle size and photoluminescence properties of submicrometer phosphors, Chem. Mater. 19 (2007) 1723–1730.
[21] V. Lojpur, S.P. Ahrenkiel, M.D. Dramicanin, Yb3+, Er3+ doped Y2O3 nanoparticles of different shapes prepared by self-propagating room temperature reaction method, Ceram. Int. 40 (2014) 16033–16039.
[22] D. Ghosh, S. Mukherjee, S. Das, High temperature oxidation behaviour of yttria (Y2O3) coated low alloy steel, Surf. Eng. 30 (2014) 524–528.
[23] F. Hayashi, M. Tanaka, D.M. Lin, M. Iwamoto, Surface structure of yttrium-modified ceria catalysts and reaction pathways from ethanol to propene, J. Catal. 316 (2014) 112–120.
[24] B. Aksakal, M. Demirel, The effect of Zirconia/Yttria/Silver substitutions on mechanostructure and cell viability of the synthesized bioceramic bone grafts, Ceram. Int. 43 (2017) 7482–7487.
[25] Y.K. Kim, H.K. Kim, G. Cho, D.K. Kim, Effect of yttria substitution on the light output of (Gd,Y)2O3:Eu ceramic scintillator, Nucl. Instrum. Methods Phys. Res. Sect. B Beam Interact. Mater. Atoms 225 (2004) 392–396.
[26] M. Cesaria, J. Collins, B. Di Bartolo, On the efficient warm white-light emission from nano-sized Y2O3, J. Lumin. 169 (2016) 574–580.

[27] S. Khanmohammadi, E. Taheri-Nassaj, Micro-porous silica-yttria membrane by sol-gel method: preparation and characterization, Ceram. Int. 40 (2014) 9403–9411.
[28] S.C. Santos, C. Yamagata, L.L. Campos, S.R.H. Mello-Castanho, Processing, microstructure and thermoluminescence response of biomorphic yttrium oxide ceramics, Ceram. Int. 42 (2016) 13291–13295.
[29] M.A. Yar, S. Wahlberg, M.O. Abuelnaga, M. Johnsson, M. Muhammed, Processing and sintering of yttrium-doped tungsten oxide nanopowders to tungsten-based composites, J. Mater. Sci. 49 (2014) 5703–5713.
[30] S. Abubakar, S. Kaya, H. Karacali, E. Yilmaz, The gamma irradiation responses of yttrium oxide capacitors and first assessment usage in radiation sensors, Sensor Actuators A Phys. 258 (2017) 44–48.
[31] C.M. Magdalane, K. Kaviyarasu, J.J. Vijaya, B. Siddhardha, B. Jeyaraj, J. Kennedy, M. Maaza, Evaluation on the heterostructured CeO2/Y2O3 binary metal oxide nanocomposites for UV/Vis light induced photocatalytic degradation of Rhodamine - B dye for textile engineering application, J Alloys Compd. 727 (2017) 1324–1337.
[32] S.F. Hassan, K.S. Tun, M. Gupta, Effect of sintering techniques on the microstructure and tensile properties of nano-yttria particulates reinforced magnesium nanocomposites, J Alloys Compd. 509 (2011) 4341–4347.
[33] B.N. Lakshminarasappa, J.R. Jayaramaiah, B.M. Nagabhushana, Thermoluminescence of combustion synthesized yttrium oxide, Powder Technol. 217 (2012) 7–10.
[34] S.C. Santos, C. Yamagata, L.L. Campos, S.R.H. Mello-Castanho, Processing and thermoluminescent response of porous biomorphic dysprosium doped yttrium disilicate burner, Mater. Chem. Phys. 177 (2016) 505–511.
[35] S.C. Santos, C. Yamagata, L.L. Campos, S.R.H. Mello-Castanho, Bio-prototyping and thermoluminescence response of cellular rare earth ceramics, J. Eur. Ceram. Soc. 36 (2016) 791–796.
[36] S.C. Santos, C. Yamagata, W. Acchar, S.R.H. Mello-Castanho, Yttria nettings by replica processing, in: Brazilian Ceramic Conference, vol. 57, 2014, pp. 798–799, 687–690.
[37] S.C. Santos, W. Acchar, C. Yamagata, S. Mello-Castanho, Yttria nettings by colloidal processing, J. Eur. Ceram. Soc. 34 (2014) 2509–2517.
[38] S.C. Santos, O. Rodrigues, L.L. Campos, Bio-prototyping of europium-yttria based rods for radiation dosimetry, Mater. Chem. Phys. 199 (2017) 557–566.
[39] S.C. Santos, O. Rodrigues Jr, L.L. Campos, EPR dosimetry of yttria micro rods, J. Alloys Compd..
[40] F.F. Lange, Densification of powder compacts: an unfinished story, J. Eur. Ceram. Soc. 28 (2008) 1509–1516.
[41] R.M. Ranson, E. Evangelou, C.B. Thomas, Modeling the fluorescent lifetime of Y2O3: Eu, Appl. Phys. Lett. 72 (1998) 2663–2664.
[42] V.V. Osipov, A.V. Rasuleva, V.I. Solomonov, Luminescence of pure yttria, Optic Spectrosc. 105 (2008) 524–530.
[43] O.M. Bordun, Influence of oxygen vacancies on the luminescence spectra of Y2O3 thin films, J. Appl. Spectrosc. 69 (2002) 430–433.
[44] V. Singh, V.K. Rai, I. Ledoux-Rak, S. Watanabe, T.K.G. Rao, J.F.D. Chubaci, L. Badie, F. Pelle, S. Ivanova, NIR to visible up-conversion, infrared luminescence, thermoluminescence and defect centres in Y(2)O(3) : Er phosphor, J. Phys. D Appl. Phys. 42 (2009).
[45] S.C. Santos, O. Rodrigues, L.L. Campos, EPR dosimetry of yttria micro rods, J. Alloys Compd. 742 (2018) 263–270.
[46] G. Xia, S. Zhou, J. Zhang, J. Xu, Structural and optical properties of YAG: Ce3+ phosphors by sol–gel combustion method, J. Cryst. Growth 279 (2005) 357–362.
[47] H.M.H. Fadlalla, C.C. Tang, YAG: Ce3+ nano-sized particles prepared by precipitation technique, Mater. Chem. Phys. 114 (2009) 99–102.
[48] A. Tannhäuser, Über die Wechselwirkung äquivalenter Erbium-Ionen in kristallinem (Er, Y)2O3, Z. Phys. 170 (1962) 533–539.
[49] C.A. Hutchison, The magnetic susceptibility of beo, Phys. Rev. 75 (1949) 465–466.